Characterizations of Cu/Sn–Zn Solder/Ag Interfaces on Photovoltaic Ribbon for Silicon Solar Cells

Kuan-Jen Chen, Fei-Yi Hung, Truan-Sheng Lui, Li-Hui Chen, and Yu-Wen Chen

***Abstract*—Sn-*x*Zn ($x = 9$, 25, and 50 wt%) alloy solders are applied in photovoltaic (PV) ribbon and connected with silicon solar cells. The interfacial microstructures, series resistance, and bonding strength of Sn-*x*Zn PV modules are investigated. Cu_5Zn_8 and $AgZn_3$ intermetallic compounds (IMCs) were found at the interfaces. The Zn content in the solder dominates the growth behavior of IMCs at the interface. The thickness of the Cu_5Zn_8 and $AgZn_3$ IMC layer increased with increasing Zn content in the solder, and thus, the series resistance of the PV module also increased. The growth of IMCs can enhance the interfacial adhesion strength, but excess Zn overconsumes the Ag electrode, reducing the bond strength of the PV module. Applying low-Zn-content Sn-*x*Zn solder to PV ribbon avoids overconsumption of the Ag layer and, thus, decreases the series resistance and internal stress.**

***Index Terms*—Bonding strength, intermetallic compounds (IMCs), internal stress, photovoltaic (PV) ribbon, Sn-*x*Zn solder.**

I. Introduction

In fact, the solar cell fabricating process is harmful to both the environment and human health because the lead-contained solders (Sn-37Pb or Sn-36Pb-2Ag) are used on commercially available photovoltaic (PV) ribbons [1], [2]. Among lead-free solders, Sn–Ag–Cu (SAC) alloy has good wettability and mechanical properties, making it suitable for solar cell interconnections [3]–[5]. The feasibility of using SAC solders in solar applications was reported in our previous studies [6], [7]. However, there is still room for improvement in SAC PV ribbon. In the electronic packaging industry, solder joint reliability is an important factor that affects the lifetime of electronic devices [8]. SAC PV ribbon reflowed on Si-based solar cells still requires using a flux, which is harmful to the environment. SAC solders containing Ag increase the PV ribbon cost. In addition, Cu_6Sn_5 and Ag_3Sn intermetallic compounds (IMCs) are formed at the SAC solder/Cu and SAC solder/Ag interfaces [5], [9]. These interfacial microstructures have high resistance and hardness and, thus, increase the internal resistance and brittleness at the interface [10].

In this study, green low-cost Sn-*x*Zn PV ribbons without flux are reflowed onto silicon solar cells to estimate their feasibility for solar module applications. The growth behaviors of IMCs at the reflowed PV module interfaces (Cu/solder and solder/Ag) are investigated. In addition, the mechanical properties of the bonding materials for PV modules are determined using the peeling force test to estimate the solderability between PV ribbon and a solar cell.

Manuscript received July 15, 2014; revised August 20, 2014 and October 24, 2014; accepted November 13, 2014. Date of publication December 8, 2014; date of current version December 18, 2014. This work was supported by the Ministry Science and Technology (MST) Instrument Center, National Cheng Kung University, and MST, Taiwan, under Grant MST 102-2221-E-006-061.

K.-J. Chen is with the Instrument Center, National Cheng Kung University, Tainan 70101, Taiwan (e-mail: kjchen1982@gmail.com).

F.-Y. Hung, T.-S. Lui, L.-H. Chen, and Y.-W. Chen are with the Department of Materials Science and Engineering, National Cheng Kung University, Tainan, 701 Taiwan (e-mail: fyhung@mail.ncku.edu.tw; luits@mail.ncku.edu.tw; chenlh@mail.ncku.edu.tw; wendy7822@hotmail.com).

Color versions of one or more of the figures in this paper are available online at http://ieeexplore.ieee.org.

Digital Object Identifier 10.1109/JPHOTOV.2014.2373822

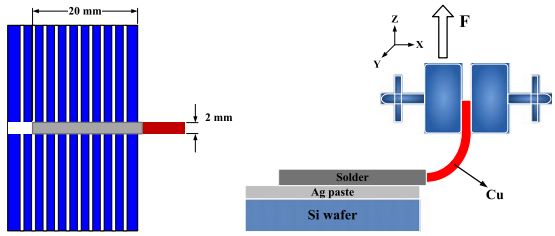

Fig. 1. Schematic diagram of peeling force test for a PV module.

II. Experimental Procedure

Sn-*x*Zn ($x = 9$, 25, and 50 wt%) alloy solders were used to fabricate the PV ribbon in this study. According to the Zn content in solder, the alloys are designated as Sn-9Zn, Sn-25Zn, and Sn-50Zn, respectively. A pure Cu ribbon (length: 100 mm; width: 2 mm; thickness: 0.2 mm) was immersed in the molten solder for 1 s to form the Sn-*x*Zn PV ribbon. In order to estimate the suitability of the Sn-*x*Zn alloy solders in the PV ribbon, the ribbons were soldered onto an Ag electrode on Si solar cells at 350 °C for 30 s. The microstructures and interfacial characteristics of the Sn-*x*Zn solders were examined using optical microscopy and high-resolution scanning electron microscopy. An electron probe microanalyzer (EPMA) was used to analyze the interfacial region of the reflowed PV ribbons. In series resistance measuring, the positive and negative of dc power supply were fed to the Ag electrode and Cu ribbon. The measurement current was increased from 0 to 10 A with an increment of 0.5 A, and the series resistance of the PV ribbons (Cu/solder/Ag) was estimated according to Ohm's law [7]. In addition, the peeling force test was used to estimate the bond strength between the PV ribbon and Si solar cell. A schematic diagram of the peeling force test for the PV module is shown in Fig. 1.

III. Results and Discussion

A. Microstructure and Interfacial Connection Characteristics

Fig. 2 shows a metallographic image of the Sn-xZn microstructures and the Sn-*x*Zn/Cu interfacial characteristics. For the solder microstructures, the alloy matrix corresponds to the Sn–Zn eutectic phase, and the needle-type structure represents

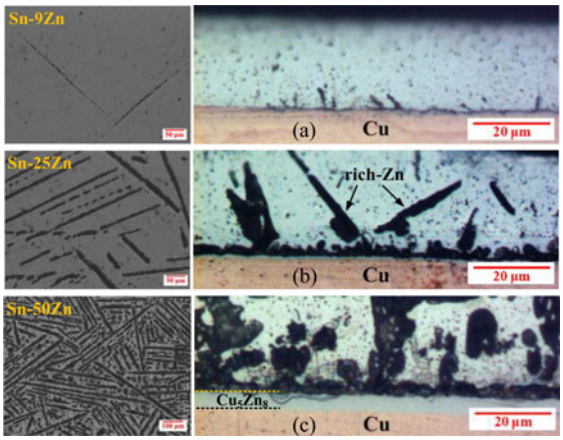

Fig. 2. Metallographic images of the microstructures of Sn-*x*Zn alloys and interfacial characteristics of PV ribbons: (a) Sn-9Zn, (b) Sn-25Zn, and (c) Sn-50Zn.

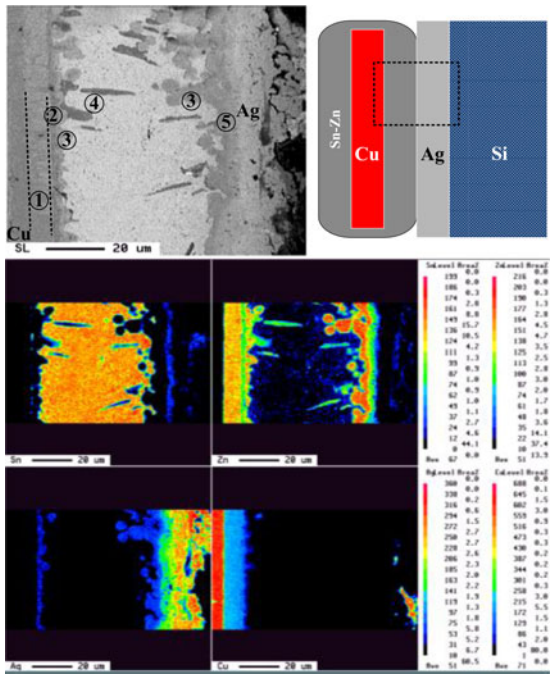

Fig. 3. EPMA images of the interfacial regions for the Sn-50Zn PV ribbon with a reflow duration of 60 s.

the primary Zn-rich phase. The area of the primary Zn-rich phase increases with increasing Zn content, and thus, the internal conductivity of the Sn-50Zn alloy was the highest [11]. The microstructure of the Sn-*x*Zn solder/Cu interface corresponds to the Zn-rich phase. With an increase in the Zn content in the solder, the discontinuous Zn-rich phase changes to a continuous layer structure. Notably, IMC layer forms at the interface between the continuous Zn-rich layer and Cu ribbon [see Fig. 2(b) and (c)]. This IMC layer corresponds to the γ-Cu_5Zn_8 phase, which is associated with the thermal diffusion reaction of solder and Cu ribbon [12], [13].

To determine the elemental (Sn, Zn, Cu, and Ag) distribution in the PV ribbon module, EPMA was used to examine the interfacial structures of the Sn-50Zn PV ribbon with a reflow duration of 60 s. As shown in Fig. 3, at the solder/Cu interface, the IMCs are layer-type γ-Cu_5Zn_8 ①, scallop-type ε-$CuZn_5$ ②, and island-type ε-$AgZn_3$ ③. In addition, the needle-type Zn-rich structure ④ grew from the interface between the IMCs and solder. At the solder/Ag paste interface, two IMCs were observed, namely ε-$AgZn_3$ ③ and layer-type ζ-AgZn ⑤. The growth mechanism of IMCs may be associated with reflow-induced thermal diffusion. The interfacial characteristics of the Sn-50Zn PV ribbon with various reflow durations were examined (see Fig. 4). The Sn–Zn eutectic phase is the main compound, with some Zn-rich phases distributed in the solder matrix. The Zn-rich phase disappeared with increasing reflow duration because the Zn-rich phase diffused into $CuZn_5$ or $AgZn_3$ during the reflow process [13]. For PV ribbon with a reflow duration of 90 s [see Fig. 4(c)], $CuZn_5$ and AgZn IMCs did not form at the Cu/solder or solder/Ag interface, which is related to thermal diffusion behavior. Briefly, a long reflow duration increases the thickness of Cu_5Zn_8 and $AgZn_3$ IMCs, which increases the internal resistance of the PV ribbon.

The interfacial microstructures of Sn-*x*Zn ($x = 9$, 25, and 50 wt%) PV ribbons obtained at a reflow duration of 30 s were examined to clarify the contribution of Zn content in the solder (see Fig. 5). It is found that the Zn-rich phase decreased with decreasing Zn content in the solder after reflow. The $AgZn_3$

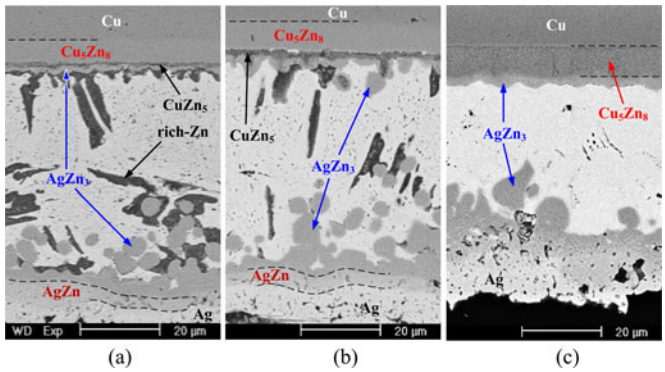

Fig. 4. Interfacial microstructures of Sn-50Zn PV ribbons with various reflow durations: (a) 30 s, (b) 60 s, and (c) and 90 s.

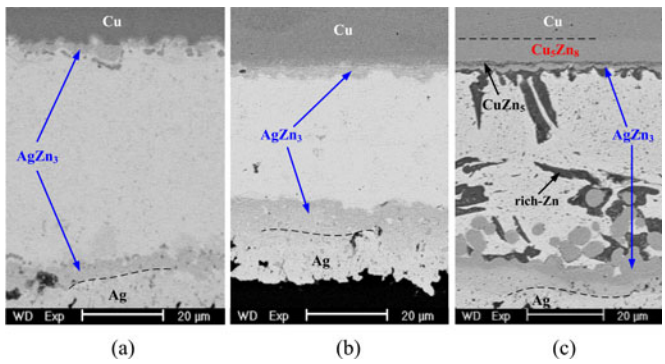

Fig. 5. Interfacial microstructures of Sn-*x*Zn PV ribbons at the reflow duration of 30 s: (a) Sn-9Zn, (b) Sn-25Zn, and (c) and Sn-50Zn.

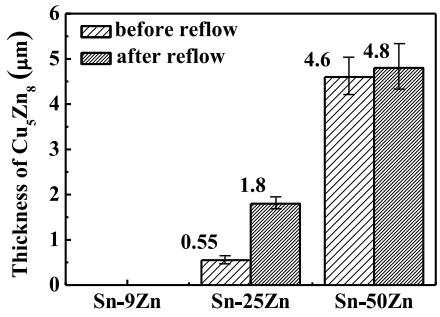

Fig. 6. Measurement of Cu_5Zn_8 thicknesses at the Cu/solder interface (before reflow indicates that Cu ribbon was immersed in molten solder to form the PV ribbon).

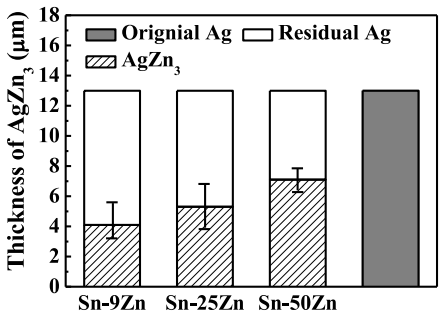

Fig. 7. Thicknesses of $AgZn_3$ and Ag paste in the interface between the Sn-*x*Zn solder and the Ag electrode.

IMC grew at the solder/Cu and solder/Ag interfaces, which is associated with the fast reaction of solder and the Ag electrode. Notably, the growth of $AgZn_3$ IMC at the solder/Ag interface affects the internal resistance and bonding characteristics of the PV ribbon module [7]. In addition, Cu_5Zn_8 IMC was only found at the Cu/Sn-25Zn solder and Cu/Sn-50Zn solder interfaces [see Fig. 5(b) and (c)], indicating that Zn content dominates the growth behavior of the Cu_5Zn_8 phase.

The thickness variations of the Cu_5Zn_8 IMC layer at the Cu/solder interface before and after reflowed are summarized in Fig. 6. For Sn-9Zn PV ribbon, whether before or after reflow, the Cu_5Zn_8 IMC layer did not form at the Cu/solder interface. The content of Zn atoms is insufficient to react with Cu for the growth of Cu_5Zn_8 IMC. The growth behavior of the Cu_5Zn_8 IMC becomes more obvious when the Zn content of the solder is increased. The reflow-induced thermal energy also promotes the growth of Cu_5Zn_8 IMC. Fig. 7 shows the variations in the Ag electrode and the $AgZn_3$ IMC thicknesses after reflow for 30 s. Compared with the original thickness of the Ag electrode ($\sim$13 μm), the residual Ag thickness of each PV ribbon decreased due to Ag fusing into the solder to form $AgZn_3$ IMC. The $AgZn_3$ thickness of Sn-9Zn PV ribbon is smaller than that those of Sn-25Zn and Sn-50Zn PV ribbons, which is attributed to the lower Zn content in the solder (and thus insufficient number of Zn atoms to react with Ag). In other words, the Zn content of the solder affects the consumption behavior of the Ag electrode at the Ag/Si interface, which dominates the series resistance of the PV module.

TABLE I
SERIES RESISTANCE OF THE PV RIBBON WITH DIFFERENT ALLOY SOLDERS

Solder	Series resistance (Ω)
Sn-9Zn	0.039
Sn-25Zn	0.035
Sn-50Zn	0.043
SAC105 [7]	0.066
SAC305 [7]	0.059

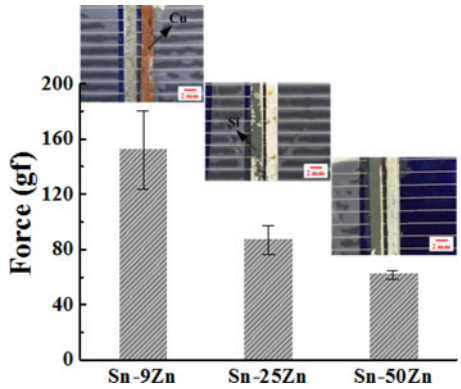

Fig. 8. Peel strength and fracture interfaces of the Sn-*x*Zn PV modules with different Zn concentration solders.

B. Effect of Intermetallic Compound Growth Behavior on Series Resistance and Bond Strength of Photovoltaic Ribbons

The interfacial IMCs (Cu_5Zn_8 and $AgZn_3$) affect the efficiency of PV ribbon on a solar cell. Therefore, the series resistance of reflowed PV ribbons was measured (see Table I). The Sn-50Zn PV ribbon has the highest series resistance (0.043 Ω), which is attributed to it having the thickest Cu_5Zn_8 (4.8 μm) and $AgZn_3$ (7.0 μm) IMCs. Notably, although Cu_5Zn_8 IMC did not form in the Sn-9Zn PV ribbon (see Fig. 6) and its residual Ag electrode is the thickest (see Fig. 7), its series resistance is not the lowest. The difference in thickness of Cu_5Zn_8 IMC and the residual Ag electrode between the Sn-9Zn and Sn-25Zn PV ribbon structures is small. In addition, the conductivity of the Sn-25Zn solder is higher than that of the Sn-9Zn solder. Therefore, the Sn-25Zn PV ribbon has the lowest series resistance (0.035 Ω). Compared with SAC PV ribbons [7], the series resistances of all Sn-*x*Zn PV ribbons are lower, which is attributed to the resistances of Cu_5Zn_8 and $AgZn_3$ IMCs being lower than those of Cu_6Sn_5 and Ag_3Sn IMCs [14]. Thus, the Sn-*x*Zn alloy solder is more suitable for PV ribbon applications.

In order to determine the quality of the PV ribbon connection to the solar cell, the peeling force test was performed (see Fig. 8). The width of the Cu ribbon (2 mm) used in this study is narrower than that of commercial Cu ribbon. Therefore, the peeling force standard for PV ribbon is 100 gf in the present study. The Sn-9Zn PV ribbon resisted the peeling force ($\sim$153 gf), meeting the standard, indicating that a thicker residual Ag layer improves bond strength. Notably, the fracture in the Sn-9Zn PV ribbon occurred at the Cu/solder interface after the peeling force test

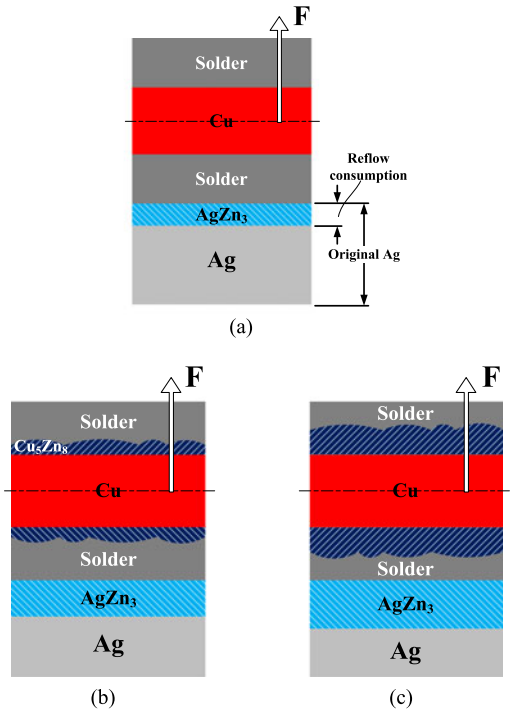

Fig. 9. Growth mechanism of interfacial IMCs in Sn-*x*Zn PV modules: (a) Sn-9Zn, (b) Sn-25Zn, and (c) and Sn-50Zn.

(see Fig. 8). In a word, lower-Zn-content solder promotes solar interconnection during the manufacture process.

Cu_5Zn_8 IMC did not form at the Cu/solder interface, and the residual Ag electrode maintained good adhesion strength [see Fig. 9(a)]. The bond strength of the Cu/solder interface is lower than that of the Ag/Si interface. For Sn-25Zn and Sn-50Zn PV ribbons, fracture did not occur at the Cu/solder interface because Zn and Cu are sufficiently interdiffused to form Cu_5Zn_8 IMC at the Cu/solder interface, enhancing the interfacial bond strength [see Fig. 9(a) and (b)]. In addition, the higher-Zn-content solder promotes Ag consumption and the formation of $AgZn_3$ IMC at the solder/Ag interface. Therefore, the bond strength of the Ag/Si interface decreased due to the different coefficients of thermal expansion, which caused internal stress at the interface between $AgZn_3$ IMC and the Ag layer [15]. Briefly, the Zn content in the Sn-*x*Zn solder affects the growth behavior of IMCs at the interface, which dominate the bond strength of the PV ribbon.

IV. Conclusion

In Sn-*x*Zn alloy solder, the Zn-rich phase dominates the internal conductivity of the solder. For the fabricated PV ribbon, Cu_5Zn_8 and $AgZn_3$ IMCs were found at the Cu/solder and solder/Ag interfaces, respectively, due to thermal diffusion behavior. The reflow duration should not be excessive as it would increase IMC thickness. High-Zn-content solder promotes the growth of IMCs and the consumption of the Ag electrode, and thus, the series resistance of the Sn-50Zn PV ribbon structure was the highest.

The IMC resistances (Cu_5Zn_8 and $AgZn_3$) for Sn-*x*Zn PV ribbons are lower than those (Cu_6Sn_5 and Ag_3Sn) for SAC PV ribbons. The series resistances of all Sn-*x*Zn PV ribbons are thus lower than those of SAC PV ribbons. Considering the reflow yield rate, lower Zn-content solder can restrain the growth of $AgZn_3$ IMC to reduce the internal stress at the interface, leading to good PV ribbon bond quality (∼153 gf) in module manufacture. The Sn-9Zn solder has potential for PV ribbon applications.

References

[1] D. R. Frear, "Microstructural evolution during thermomechanical fatigue of 62Sn-36Pb-2Ag and 60Sn-40Pb solder joints," *IEEE Trans. Compon., Hybrids Manuf. Technol.*, vol. 13, no. 4, pp. 718–726, Aug. 1990.

[2] Y. T. Chiu, K. L. Lin, and Y. S. Lai, "Orientation transformation of Pb rains in 5Sn-95Pb/63Sn-37Pb composite flip-chip solder joints during electromigration test," *J. Mater. Res.*, vol. 23, no. 7, pp. 1877–1881, Jul. 2008.

[3] H. A. A. M. Amin, D. A. Shnawah, S. M. Said, M. F. M. Sabri, and H. Arof, "Effect of Ag content and the minor alloying element Fe on the electrical resistivity of Sn-Ag-Cu solder alloy," *J. Alloy. Compounds*, vol. 599, no. 25, pp. 114–120, Jun. 2014.

[4] H. J. Ji, Q. Wang, M. Y. Li, and C. Q. Wang, "Ultrafine-grain and isotropic Cu/SAC305/Cu solder interconnects fabricated by high-intensity ultrasound-assisted solidification," *J. Electron. Mater.*, vol. 43, no. 7, pp. 2467–2478, Apr. 2014.

[5] C. Y. Yu, J. Lee, W. L. Chen, and J. G. Duh, "Enhancement of the impact toughness in Sn-Ag-Cu/Cu solder joints via modifying the microstructure of solder alloy," *Mater. Lett.*, vol. 119, no. 15, pp. 20–23, Mar. 2008.

[6] K. J. Chen, F. Y. Hung, T. S. Lui, L. H. Chen, D. W. Qiu, and T. L. Chou, "Effects of electrical current on microstructure and interface properties of Sn-Ag-Cu/Ag photovoltaic ribbons," *Mater. Trans.*, vol. 54, no. 7, pp. 1155–1159, Jun. 2013.

[7] K. J. Chen, F. Y. Hung, T. S. Lui, L. H. Chen, D. W. Qiu, and T. L. Chou, "Microstructure and electrical mechanism of Sn-xAg-Cu PV-ribbon for solar cells," *Microelectron. Eng.*, vol. 116, no. 25, pp. 33–39, Oct. 2014.

[8] J. H. L. Pang, D. Y. R. Chong, and T. H. Low, "Thermal cycling analysis of flip-chip solder joint reliability," *IEEE Trans. Compon., Packag., Technol.*, vol. 24, no. 4, pp. 705–712, Dec. 2001.

[9] M. L. Huang, F. Yang, N. Zhao, and Y. C. Yang, "Synchrotron radiation real-time in situ study on dissolution and precipitation of Ag_3Sn plates in sub-50 μm Sn-Ag-Cu solder bumps," *J. Alloy. Comp.*, vol. 602, no. 25, pp. 281–284, Mar. 2014.

[10] W. R. Osorio, L. C. Peixoto, L. R. Garcia, A. Garcia, and J. E. Spinelli, "The effects of microstructure and Ag_3Sn and Cu_6Sn_5 intermetallics on the electrochemical behavior of Sn-Ag and Sn-Cu solder alloys," *Int. J. Electrochem. Sci.*, vol. 7, pp. 6436–6452, Jul. 2012.

[11] G. A. Lan, T. S. Lui, and L. H. Chen, "The role of eutectic phase and acicular primary crystallized Zn phase on electrification-fusion induced fracture of Sn-xZn solder alloys," *Mater. Trans.*, vol. 52, no. 11, pp. 2111–2118, 2011.

[12] K. L. Lin and C. L. Shih, "Wetting interaction between Sn-Zn-Ag solders and Cu," *J. Electron. Mater.*, vol. 32, no. 2, pp. 95–100, 2003.

[13] C. S. Lee and F. S. Shieu, "Growth of intermetallic compounds in the Sn-9Zn/Cu joint," *J. Electron. Mater.*, vol. 35, no. 8, pp. 1660–1664, Mar. 2006.

[14] P. L. Rossiter, *The Electrical Resistivity of Metals and Alloys*. London, U.K.: Arnold, 1977.

[15] T. C. Chang, M. H. Hon, and M. C. Wang, "Adhesion strength of the Sn-9Zn-xAg/Cu interface," *J. Electron. Mater.*, vol. 32, no. 6, pp. 516–522, Jan. 2003.

Authors' photographs and biographies not available at the time of publication.